

Unbiased high-dimensional flow cytometry identified NK and DC immune cell signature in Luminal A-type and triple negative breast cancer

Lukas Heger^a, Gordon F. Heidkamp^{a#}, Lukas Amon^a, Falk Nimmerjahn^b, Tobias Bäuerle^c, Andreas Maier^d, Ramona Erber^{e,f}, Arndt Hartmann^{e,f}, Carolin C. Hack^{f,g}, Matthias Ruebner^{f,g}, Hanna Huebner^{f,g}, Peter Fasching^{f,g}, Matthias W. Beckmann^{f,g}, and Diana Dudziak^{a,f,h,i,j,k}

^aDepartment of Dermatology, Laboratory of Dendritic Cell Biology, University Hospital Erlangen, Friedrich-Alexander-Universität Erlangen-Nürnberg, Erlangen, Germany; ^bChair of Genetics, Friedrich-Alexander-Universität Erlangen-Nürnberg, Erlangen, Germany; ^cInstitute of Radiology, University Hospital Erlangen, Friedrich-Alexander-Universität Erlangen-Nürnberg, Erlangen, Germany; ^dChair of Computer Science 5 (Pattern Recognition), Friedrich-Alexander-Universität Erlangen-Nürnberg, Erlangen, Germany; ^eInstitute of Pathology, University Hospital Erlangen, Friedrich-Alexander-Universität Erlangen-Nürnberg, Erlangen, Germany; ^fComprehensive Cancer Center Erlangen-European Metropolitan Area of Nuremberg (CCC ER-EMN), Erlangen, Germany; ^gDepartment of Gynecology and Obstetrics, University Hospital Erlangen, Friedrich-Alexander-Universität Erlangen-Nürnberg, Erlangen, Germany; ^hFAU Profile Center Immunomedicine (FAU I-MED), Friedrich-Alexander-Universität Erlangen-Nürnberg, Erlangen, Germany; ⁱDeutsches Zentrum Immuntherapie (DZI), Erlangen, Germany; ^jInstitute of Immunology, Jena University Hospital, Friedrich-Schiller-University, Jena, Germany; ^kComprehensive Cancer Center Central Germany Jena/Leipzig, Jena, Germany

ABSTRACT

Breast cancer is the most common malignancy in women worldwide and a highly heterogeneous disease. Four different subtypes are described that differ in the expression of hormone receptors as well as the growth factor receptor HER2. Treatment modalities and survival rate depend on the subtype of breast cancer. However, it is still not clear which patients benefit from immunotherapeutic approaches such as checkpoint blockade. Thus, we aimed to decipher the immune cell signature of the different breast cancer subtypes based on high-dimensional flow cytometry followed by unbiased approaches. Here, we show that the frequency of NK cells is reduced in Luminal A and B as well as triple negative breast cancer and that the phenotype of residual NK cells is changed toward regulatory CD11b⁻CD16⁻ NK cells. Further, we found higher frequencies of PD-1⁺ CD4⁺ and CD8⁺ T cells in triple negative breast cancer. Moreover, while Luminal A-type breast cancer was enriched for CD14⁺ cDC2 (named type 3 DC (DC3)), CD14⁻ cDC2 (named DC2) were more frequent in triple negative breast cancer. In contrast, HER2-enriched breast cancer did not show major alterations in the composition of the immune cell compartment in the tumor microenvironment. These findings suggest that patients with Luminal A- and B-type as well as triple negative breast cancer might benefit from immunotherapeutic approaches targeting NK cells.

ARTICLE HISTORY

Received 30 August 2023
Revised 7 December 2023
Accepted 14 December 2023


KEYWORDS

Breast cancer; immune cell signature; NK cells; PD-1; tumor microenvironment


Introduction

Breast cancer (BC) is the most common malignancy in women worldwide. Four different subtypes of BC are differentiated based on the expression of the hormone receptor (HR), estrogen receptor (ER), progesterone receptor (PR), status of human epidermal growth factor receptor 2 (HER2) as well as grading. These are Luminal A (HR⁺; HER2⁻, G1/2) and B (HR⁺; HER2⁻, G3), HER2-enriched (HR[±]; HER2⁺), and triple negative BC (TNBC; HR⁻; HER2⁻)^{1,2}. The subtype of breast cancer is associated with overall survival of the patients: While patients with Luminal A-type BC have a more favorable prognosis, patients with TNBC have a worse prognosis^{3,4}. Irrespective of the molecular subtype of BC, lymphocyte infiltration is a prognostic factor for disease-free survival and pathological complete response (pCR)^{5–7}. On average, 20% of TN and 16% of HER2-enriched BC show lymphocyte-predominant BC (>50% infiltrating lymphocytes), whereas this is less frequent in HR⁺ BC^{8,9}. Moreover, an increase of 10% of infiltrating

lymphocytes reduces the risk of relapse and death⁶. Further, the type of infiltrating lymphocytes is associated either with favorable or worse prognosis^{10,11}: Infiltration with CD8⁺ cytotoxic T cells is beneficial, while infiltration with FOXP3⁺ regulatory T cells is accompanied with a poor prognosis^{8,12–15}. Here as well, the molecular subtypes of BC differ, as TN and HER2⁺ BC show higher infiltration with both CD8⁺ as well as regulatory T cells compared to HR⁺ BC⁸. In addition, presence of NK cells and recruitment of conventional dendritic cells (cDC) type 1 (cDC1) have been shown to be beneficial for overall survival in breast cancer^{16,17}. However, most studies phenotyping immune cell infiltration in breast cancer either rely on immunohistochemical analysis of patient samples, which only allow for the analysis of few markers or bulk RNA-sequencing of cancer tissue not enabling single-cell resolution^{5,11,18–20}. Therefore, differentiation of rather complex cell populations is difficult as it requires several markers stained simultaneously. Thus, we aimed to develop a workflow using high-

CONTACT Diana Dudziak  diana.dudziak@med.uni-jena.de; lukas.heger@uk-erlangen.de  Department of Dermatology, Laboratory of Dendritic Cell Biology, University Hospital Erlangen, Friedrich-Alexander-Universität Erlangen-Nürnberg, Erlangen 91052, Germany; Institute of Immunology, Jena University Hospital, Friedrich-Schiller-University, Jena 07743, Germany

[#]Roche Innovation Center Munich, Munich, Germany.

 Supplemental data for this article can be accessed online at <https://doi.org/10.1080/2162402X.2023.2296713>.

© 2023 The Author(s). Published with license by Taylor & Francis Group, LLC.

This is an Open Access article distributed under the terms of the Creative Commons Attribution-NonCommercial License (<http://creativecommons.org/licenses/by-nc/4.0/>), which permits unrestricted non-commercial use, distribution, and reproduction in any medium, provided the original work is properly cited. The terms on which this article has been published allow the posting of the Accepted Manuscript in a repository by the author(s) or with their consent.

dimensional flow cytometry to identify changes in the immune cell signature of breast cancer subtypes. Using unbiased approaches, we identified clusters of immune cells that changed between unaffected and breast cancer tissue as well as specifically in certain subtypes of breast cancer. Thereby, we could show that especially the phenotype of NK cells is altered in Luminal A-type as well as in TNBC toward regulatory NK cells. Our data further revealed an enrichment of PD-1⁺ CD4⁺ and CD8⁺ T cells in TNBC.

Material and methods

Patient selection

Between February 2017 and May 2020, a total of 43 breast cancer patients were selected for tissue sampling with a clinical tumor size of cT2 or higher to get adequate tissue for routine diagnostic

and further analysis. All patients took part in the iMODE-B study (“Imaging and Molecular Detection of Breast Cancer”) which was approved by the Ethikkommission der Friedrich-Alexander-Universität Erlangen-Nürnberg (#325_19 B). After signature of written informed consent in accordance with the Declaration of Helsinki, patients underwent breast conserving surgery or mastectomy (Figure 1). The interval between initial biopsies for diagnostics and biopsies during surgery was 30 d (± 16) for patients without neoadjuvant therapy and 169 d (± 59 d) for patients with neoadjuvant therapy.

Processing of breast cancer and surrounding unaffected tissue

Biopsies of breast cancer patients were taken after breast conserving surgery or mastectomy at the Department of

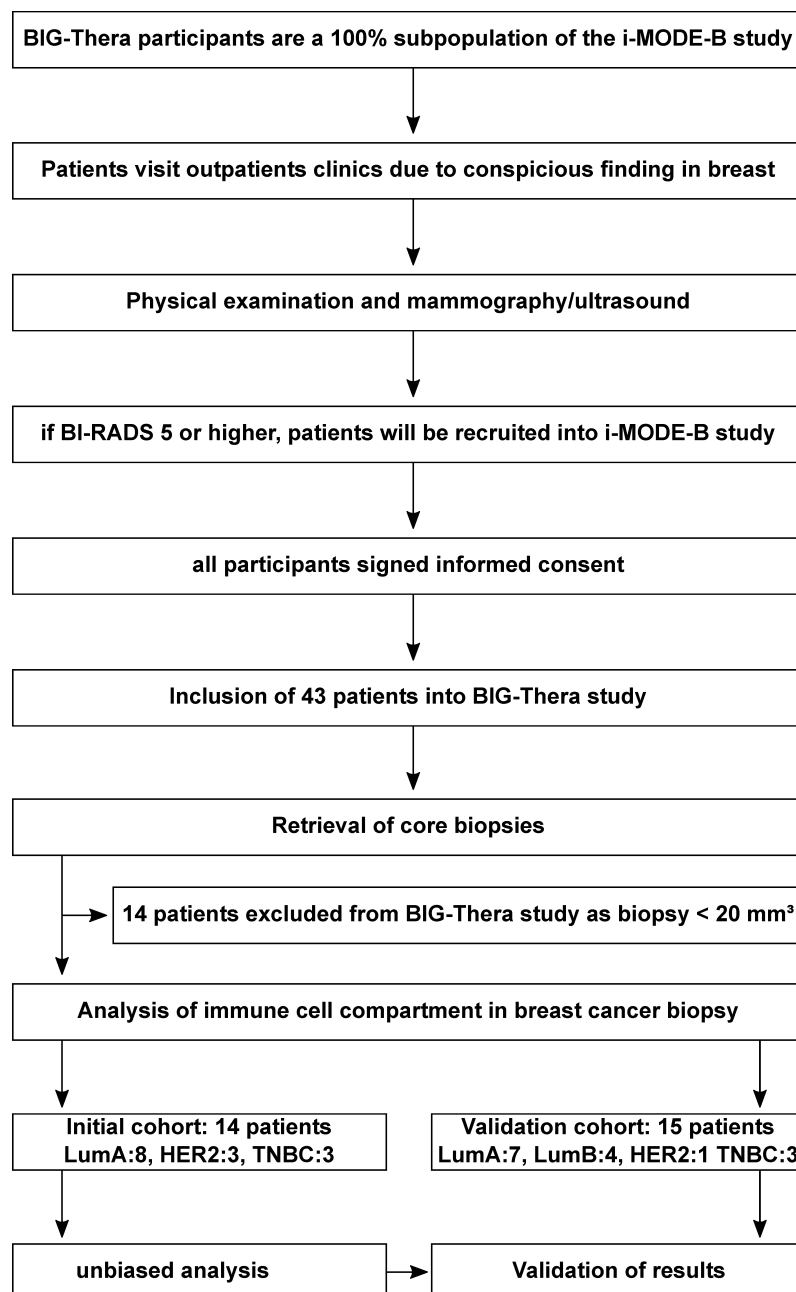


Figure 1. Overview of procedures for inclusion of participants for BIG-Thera study.

Gynecology and Obstetrics of the University Hospital Erlangen by a pathologist (Institute of Pathology, University Hospital Erlangen) before formalin fixation and stored in 1× PBS at 4–8°C until further examination. Due to the size of the samples and the expected cell yield, 14 samples were excluded from flow cytometric analysis. These samples were embedded in O.C. T. and stored at -80°C as described before (Figure 1).

For flow cytometric analysis, single-cell suspensions of the tissue of the remaining 29 patients were prepared (Table 1). Therefore, tissue was minced using scalpel and forceps into small cubes, transferred to a 50 ml tube and incubated in 5 ml RPMI with 2% human sera, 150 U/ml Collagenase D and 20 µg/ml DNase I for 20 min at 37°C. After grinding over a 100 µm cell strainer using a pestle to increase the cell yield, the

sample was centrifuged with 520 × g for 5 min at 4°C. After resuspension in 10 ml of RPMI, cells were again filtered over a 100 µm cell strainer. Subsequently, single-cell suspensions were used for flow cytometric analysis.

Flow cytometric analysis

Up to 5 × 10⁶ cells were transferred into a well of a 96-well plate (V-bottom). The cells were centrifuged for 5 min with 520 × g at 4°C. After washing with PBS + 2% human serum (FACS buffer), cells were stained with fluorochrome-coupled antibodies diluted in FACS buffer according to Table 2 (initial cohort) or Table S1 (validation cohort). Cells were resuspended in 100 µl of the antibody staining mix and incubated for 30 min

Table 1. Cohort of patients analyzed for immune cell populations in breast cancer and surrounding unaffected tissue.

		All (N=29) mean (sd) or n (%)	Initial (N=14) mean (sd) or n (%)	Validation (N=15) mean (sd) or n (%)
age		64 (15.5)	64 (15.0)	64 (16.4)
T	2	22 (75.9%)	11 (78.6%)	11 (73.3%)
	3	1 (3.4%)	0 (0%)	1 (6.7%)
	4	6 (20.7%)	3 (21.4%)	3 (20.0%)
N	0	20 (69%)	10 (71.4%)	10 (66.7%)
	1	9 (31%)	4 (28.6%)	5 (33.3%)
M	0	23 (79.3%)	11 (78.6%)	12 (80.0%)
	1	1 (3.4%)	0 (0%)	1 (6.7%)
	X	5 (17.2%)	3 (21.4%)	2 (13.3%)
G	1/2	16 (55.2%)	9 (64.3%)	7 (46.7%)
	3	12 (41.4%)	5 (35.7%)	7 (46.7%)
ER	positive	21 (72.4%)	10 (71.4%)	11 (73.3%)
	negative	8 (27.6%)	4 (28.6%)	4 (26.7%)
PR	positive	17 (58.6%)	7 (50%)	8 (53.3%)
	negative	12 (41.4%)	7 (50%)	7 (46.7%)
HER2	positive	4 (13.8%)	3 (21.4%)	1 (6.7%)
	negative	25 (86.2%)	11 (78.6%)	14 (93.3%)
Molecular-like subtype	LumA	15 (51.7%)	8 (57.4%)	7 (46.7%)
	LumB	4 (13.8%)	0 (0%)	4 (26.7%)
	HER2+	4 (13.8%)	3 (21.4%)	1 (6.7%)
	TNBC	6 (20.7%)	3 (21.4%)	3 (20.0%)
Pretreat-ment	Chemotherapy (CT)	4 (13.8%)	1 (7.1%)	3 (20.0%)
	anti-HER2+CT	3 (10.3%)	2 (14.3%)	1 (6.7%)
	others	1 (3.4%)	0 (0%)	1 (6.7%)
	no	21 (72.4%)	11 (78.6%)	10 (66.7%)

T: Tumor size; N: Lymph node spreading; M: Metastasis; G: Grading

Table 2. Antibody staining panel for identification of immune cells in breast cancer and surrounding unaffected tissue.

Fluorochrome	Antigen	Clone	Isotype	Dilution
BUV395	CD3	UCHT1	Mouse IgG1, κ	1:50
BUV737	CD8	SK1	Mouse IgG1, κ	1:100
BV421	CD56	5.1H11	Mouse IgG1, κ	1:100
BV421	NKp46	9E2	Mouse IgG1, κ	1:100
BV510	CD45	HI30	Mouse IgG1, κ	1:50
BV570	CD16	3G8	Mouse IgG1, κ	1:50
BV605	CD19	SJ25C1	Mouse IgG1, κ	1:100
BV605	CD20	2H7	Mouse IgG2b, κ	1:100
BV650	CD123	6H6	Mouse IgG1, κ	1:100
BV711	CD141	1A4	Mouse IgG1, κ	1:100
A488	CD279 (PD-1)	EH12.2H7	Mouse IgG1, κ	1:100
PerCP/Cy5.5	CD303	201A	Mouse IgG2a, κ	1:100
PE	CD4	RPA-T4	Mouse IgG1, κ	1:100
PE-CF594	HLA-DR	G46-6	Mouse IgG2a, κ	1:200
PE/Cy5	CD11b	M1/70	Rat IgG2b, κ	1:1,000
PE/Cy7	CD11c	3.9	Mouse IgG1, κ	1:100
A647	CD1c	L161	Mouse IgG1, κ	1:100
A700	CD14	HCD14	Mouse IgG1, κ	1:100
APC/Cy7	CD324 (E-Cadherin)	67A4	Mouse IgG1, κ	1:100
APC/Cy7	CD326 (EpCAM)	G8.8	Rat IgG2a, κ	1:100
APC/Cy7	CD340 (erbB2/HER-2)	24D2	Mouse IgG1, κ	1:100

on ice. After washing twice with 100 μ l FACS buffer, cells were resuspended in DAPI-containing FACS buffer (1:10,000) and samples acquired using a BD LSRFortessa. After acquisition, samples were analyzed using FlowJo (BD Biosciences, V10). To allow for an unbiased analysis, all flow cytometry samples were merged using the concatenate function. The retrieved file containing all data was analyzed using the UMAP algorithm to reduce the complexity of the data set and to cluster the cells in a two-dimensional space²¹. Then, X-shift was used to identify cell clusters based on KNN density estimation²². Statistical analysis was performed with GraphPad Prism (Two-group comparisons: Student's t test; Multi-group comparisons: One-way ANOVA with Dunnett's multiple-comparison test). As for unbiased analysis using UMAP, samples have to be acquired during a short amount of time using the same LOTs for different antibodies to reduce variety based on the flow cytometer itself, the received biopsies were classified into an initial cohort (14 patients between February and July 2018; see Table 1) and a validation cohort (15 patients; see Table 1).

Results

Breast cancer consists of different intrinsic molecular subtypes that differentially respond to therapy as well as show differences in overall and recurrence free survival^{23,24}. As this might also be influenced by the immune cell compartment present in the tumor microenvironment, we were interested in differences in the immune cell signatures of different subtypes of breast cancer. Therefore, we received samples of breast cancer as well as surrounding unaffected tissue from patients undergoing surgery at the University Hospital Erlangen in order to analyze the composition of the immune cell compartment (Figure S1, Table 1). Biopsies received between February and July 2018 were used for unbiased analysis of the immune cell compartment using high-dimensional flow cytometry (Initial cohort, Table 1).

Single-cell suspensions were stained with a panel of 21 fluorochrome-coupled antibodies covering a multitude of immune cell populations (Table 2). After flow cytometric acquisition of the samples, we first identified immune cells by gating for CD45⁺ cells, which were alive and negative for tumor cell markers (Figure 2a). Overall, we observed that immune cells were significantly enriched in the BC microenvironment compared to unaffected surrounding tissue (Figure 2b). In order to perform the unbiased analysis, we merged the samples using the concatenate function and used the UMAP algorithm to reduce the complexity of the data set and to cluster the cells in a two-dimensional space (Figure 2c). Due to merging of the samples into one file, we retrieved one UMAP allowing the direct comparison of all samples. Using X-shift, we identified 22 cell clusters based on KNN density estimation, which were present both in unaffected and breast cancer tissue (Figure 2c,d).

In order to analyze changes between unaffected and breast cancer tissue, we determined changes in the composition of the identified clusters between unaffected and breast cancer tissue (Figure 2e and Figure S2). We found that four clusters showed significant changes between unaffected and breast cancer tissue with cluster 1, 3, and 7 being enriched in breast cancer tissue, while cluster 21 was decreased compared to unaffected tissue (Figure 2e). As some of the patients were pretreated with

neoadjuvant chemotherapy (CT) prior to surgery, we also tested whether the chemotherapy had an influence on the composition of the immune cell compartment in breast cancer tissue (Figure 2f and Figure S3). Indeed, cluster 11 and 21 were enriched in breast cancer tissue of patients treated with neoadjuvant CT (\pm Trastuzumab, Pertuzumab), while cluster 22 was decreased (Figure 2f). Thus, our unbiased analysis was able to identify changes in the immune cell compartment in BC tissue as well as in patients treated with chemotherapy compared to untreated patients.

In addition to general differences in the immune cell compartment, we were also interested in BC-subtype specific alterations. Therefore, we determined which clusters were changed in HER2-enriched, Luminal A-type, and TNBC as well as whether CD45⁺ immune cells were enriched in BC tissue (Figure 3a,b). Overlaying representative samples with the identified clusters showed strong differences in the immune cell compartment, especially in TNBC (Figure 3a). Further, TNBC showed a strong increase in CD45⁺ immune cells (Figure 3b). While immune cells in Luminal A-type BC were not enriched compared to the unaffected tissue of all patients, they were significantly enriched when a paired comparison of BC and unaffected tissue in the same patient was performed (Figure 3b). Comparing the frequency of the different clusters between unaffected tissue and the different subtypes showed that clusters 2, 5, and 6 were enriched in TNBC (Figure 3c and Figure S3). Further, Luminal A-type BC showed an increase in cluster 7, 10, and 19, while cluster 21 was significantly decreased in Luminal A-type BC (Figure 3c). Thus, especially TNBC and Luminal A-type BC show differences in frequency and composition of the immune cells in the tumor microenvironment, which might influence their response to therapies.

In order to determine which cell types were altered in the BC microenvironment, we used ClusterExplorer to analyze the different clusters in more detail (Figure 4). Based on the relative expression of these markers, we assigned each cluster to a certain immune cell population (Figure 4). Cluster 1, enriched in breast cancer tissue, represented NK cells as they expressed CD56 and/or NKp46 but were negative for CD3²⁵. However, they were negative for CD16, an important effector molecule expressed on NK cells (Figure 4). Cluster 3 (enriched in BC) contained $\gamma\delta$ or DN T cells expressing CD3 (T cells) but lacking the expression of both CD4 and CD8 as well as of CD56 and/or NKp46. Cluster 5 and 6, which were overrepresented in TNBC, showed enhanced expression of CD3, PD-1 as well as CD8 and CD4, respectively. Thus, these cells showed a phenotype of exhausted CD8⁺ (Cluster 5) or CD4⁺ (Cluster 6) T cells (Figure 4). Cluster 7, which was enriched in Luminal A-type BC, displayed high expression of CD1c, CD11c, and HLA-DR, which corresponds to the dendritic cell (DC) subpopulation cDC2 (Figure 4). Cluster 10 was also enriched in Luminal A-type BC and represented B cells based on the expression of CD19/CD20 as well as HLA-DR (Figure 4). Further, Cluster 19 (enriched in Luminal A) exhibited marker expression reminiscent of CD8⁺ T cells, while Cluster 21 (overall decreased in BC as well as in Luminal A-type BC) consisted of NK cells expressing both CD11b and CD16 (Figure 4). Thus, our unbiased analysis revealed that

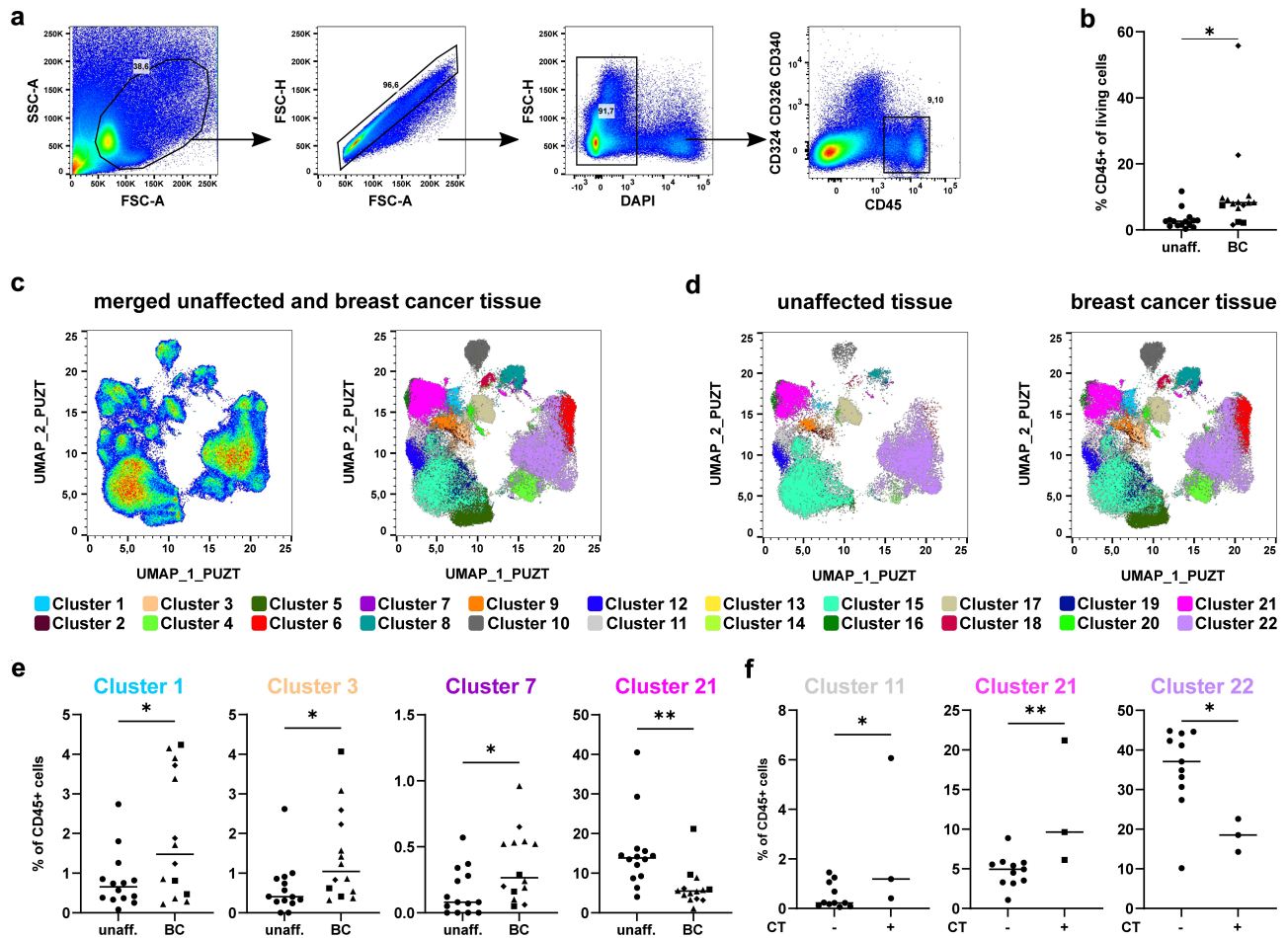


Figure 2. High-dimensional analysis of the immune cell signature in breast cancer tissue using unbiased approaches. Single cell suspensions of breast cancer samples and unaffected tissue of the same patients were stained with a panel of 21 fluorochrome-coupled monoclonal antibodies. Cells were acquired using a BD LSRFortessa and analyzed using FlowJo (version 10, BD Biosciences). a) Gating strategy to identify CD45⁺ immune cells in the samples of breast cancer patients. After gating for the morphology of cells (FSC-A/SSC-A), doublets (FSC-A/FSC-H), dead cells (DAPI⁺) and cancer cells (CD324/CD326/CD340⁺) were excluded. Then, CD45⁺ immune cells were selected and the frequency among all viable cells determined. b) Scatter plot shows frequency of CD45⁺ immune cells among all viable cells for all breast cancer samples as well as unaffected surrounding tissue of the same patient (Student's t-test; * $p < 0.05$, ** $p < 0.01$). c) UMAP analysis and overlay with cell clusters identified using X-Shift are shown as dot plot for merged sample. d) The merged samples were split up into unaffected and breast cancer tissue. Dot plots show the results of the UMAP analysis overlaid with the identified clusters using X-Shift. e) Frequency of each cluster among the CD45⁺ immune cells was determined. Scatter plots show clusters that differ significantly between unaffected and breast cancer tissue (Student's t-test; * $p < 0.05$, ** $p < 0.01$). f) Breast cancer samples were grouped into untreated and chemotherapy (CT)-treated samples. Scatter plots show clusters that differ significantly between treated and untreated breast cancer samples (Student's t-test; * $p < 0.05$, ** $p < 0.01$).

mainly frequencies of NK cells, T cells, B cells, and DCs are altered in BC.

In order to verify the unbiased results of our initial cohort of patients, we included further samples of BC patients (Validation cohort, Table 1). We then analyzed immune cell populations showing alterations in the unbiased approach, such as NK cells, T cells, B cells, and DCs, by using established gating strategies. First, for the analysis of NK cells, we excluded cells expressing T cell (CD3) as well as B cell (CD19 and CD20) markers (Figure S5A). In the remaining cells, we selected cells expressing the pan-NK cell markers CD56 and/or NKp46, which were negative for the myeloid cell marker CD14 (Figure S5A). Then, we determined the frequency of (CD56/NKp46)⁺ NK cells among all CD45⁺ immune cells (Figure 5a) as well as analyzed the expression of CD11b and CD16 on the identified NK cells as these were differentially expressed on the cells present in clusters 1 and 21, which were altered in BC tissue compared to the unaffected surrounding tissue (Figures 2–4). The frequency of NK cells among CD45⁺ immune cells

was significantly decreased in Luminal A- and B-type BC as well as in TNBC (Figure 5a). When we analyzed the phenotype of the NK cells present in unaffected surrounding tissue, they were primarily double-positive for CD16 as well as CD11b (Figure 5b). In contrast, CD11b⁺CD16⁺ NK cells were significantly decreased in Luminal A-type and HER2-enriched BC as well as in TNBC (Figure 5b). Further, CD11b[−]CD16[−] NK cells were enriched in Luminal A-type and TNBC (Figure 5b).

As the unbiased analysis revealed changes in the T cell compartment (cluster 2, 3, 5, 6, and 19), we also performed conventional gating for T cell subsets (Figure S5B). Among the CD45⁺ immune cells, we selected CD3⁺(CD19/CD20)[−] T cells, which were divided into (CD56/NKp46)⁺ NKT cells as well as in (CD56/NKp46)[−] conventional T cells. Among the (CD56/NKp46)[−] T cells, cells were divided into CD4⁺ T cells, CD8⁺ T cells as well as in CD4[−]CD8[−] (DN) T cells (Figure S5B). The frequency of T cells as well as the different subtypes among CD45⁺ immune cells were not altered in BC compared to unaffected surrounding tissue (Figure 5c,d), but TNBC showed

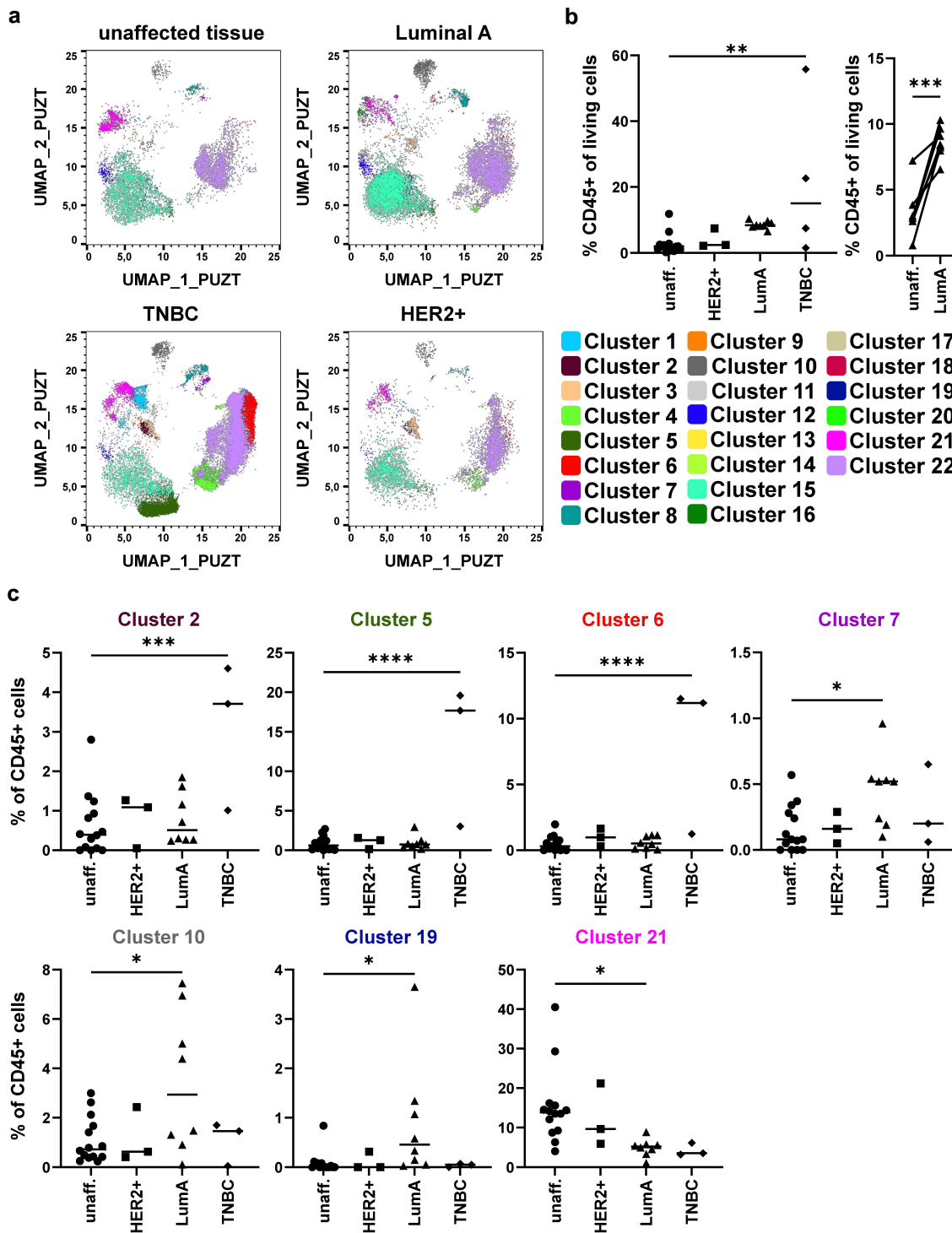


Figure 3. Identification of subtype-specific immune cell alterations in breast cancer samples. a) Merged samples from Figure 2 were split up into the original files after UMAP and X-Shift analysis. Dot plots show a representative donor for unaffected tissue, Luminal A-type BC, HER2-enriched (HER2+) BC, and TNBC. Dot plots were overlaid with the identified clusters by X-Shift and color-coded according to Figure 2. b) Scatter plot shows the frequency of CD45⁺ immune cells among all viable cells (determined for each sample as in Figure 2a; one-way ANOVA with Dunnett's multiple comparison test; * $p < 0.05$, ** $p < 0.01$, *** $p < 0.001$, **** $p < 0.0001$). c) Frequency of each cluster among CD45⁺ immune cells in each tissue sample were determined and plotted as scatter plot. Shown are clusters displaying significant differences between unaffected tissue and one of the analyzed BC subtypes (one-way ANOVA with Dunnett's multiple comparison test; * $p < 0.05$, ** $p < 0.01$, *** $p < 0.001$, **** $p < 0.0001$).

lower infiltration with CD8⁺ T cells compared to HER2-enriched BC (Figure 5d). As cluster 19, which was enriched in Luminal A-type BC, showed an expression profile of CD11c⁺CD8⁺ T cells (Figure 4), we determined the frequency of CD11c⁺CD8⁺ T cells (Figure 5e). Indeed, we could verify that CD11c⁺CD8⁺ T cells were enriched in Luminal A-type BC

compared to unaffected tissue (Figure 5e). Further, specifically in TNBC, CD4⁺ and CD8⁺ T cells showed enhanced expression of PD-1 (Figure 5f) and a higher frequency of CD4⁺ and CD8⁺ T cells were positive for PD-1 compared to unaffected surrounding tissue (Figure 5g). As with Cluster 10 also B cells were affected in Luminal A-type BC, we further determined

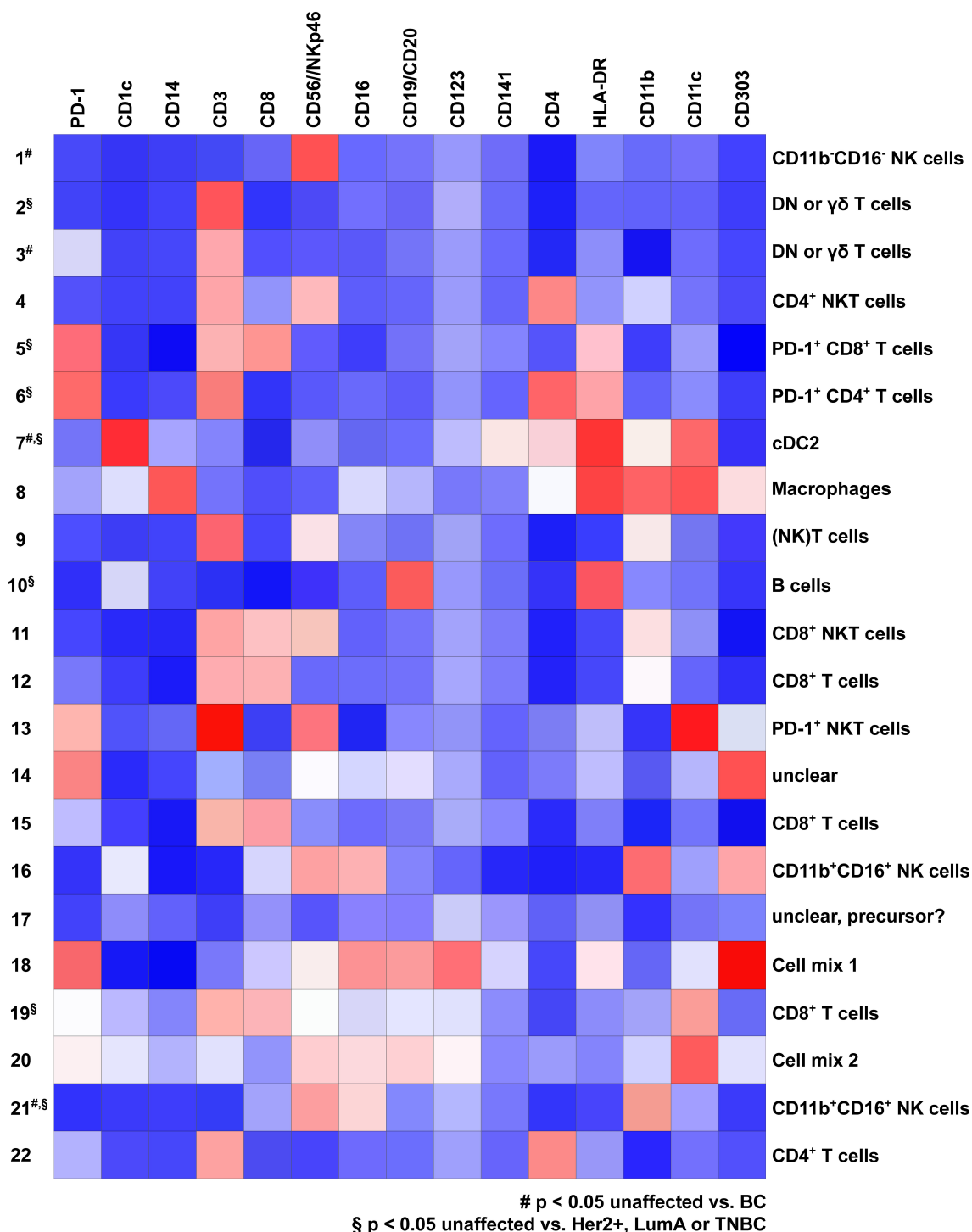


Figure 4. Identification of immune cell phenotype in X-Shift clusters using ClusterExplorer. Cells contained in the 22 clusters identified by X-Shift analysis in the merged file containing all 14 BC and 14 unaffected tissue samples were analyzed for the expression of the stained markers using the FlowJo plugin ClusterExplorer and plotted as heatmap. Heatmap depicts the expression of the 17 markers used for the identification of the X-Shift clusters. Dependent on the expression pattern, cells were assigned to the indicated cell populations on the right side of the heatmap. Signal intensity is color coded from blue (low expression) to red (high expression).

frequency of $(CD19/CD20)^+HLA-DR^+$ B cells in our cohort. Indeed, the tumor microenvironment of Luminal A-type BC showed an enrichment for B cells compared to unaffected surrounding tissue (Figure 5h).

Lastly, we attempted to validate the changes in the DC compartment by gating for cDC2 (Figure S5C). In the $CD45^+$ immune cell compartment, we selected $CD3^-(CD19/CD20)^-$ cells followed by gating for $HLA-DR^+(CD56/CD335)^-$ antigen-

presenting cells (APCs). In the APC compartment, we gated for $CD1c^+CD11c^+$ cDC2 (Figure S5C). As DCs are rather scarce, we included only samples with a final cell count for $cDC2 > 50$ into the analysis. Here, we could not observe significant differences between unaffected surrounding tissue and Luminal A-type or TNBC (Figure 5i). However, it was recently reported that cDC2 can be differentiated into subpopulations called DC2 and DC3, which differ in the expression of CD5,

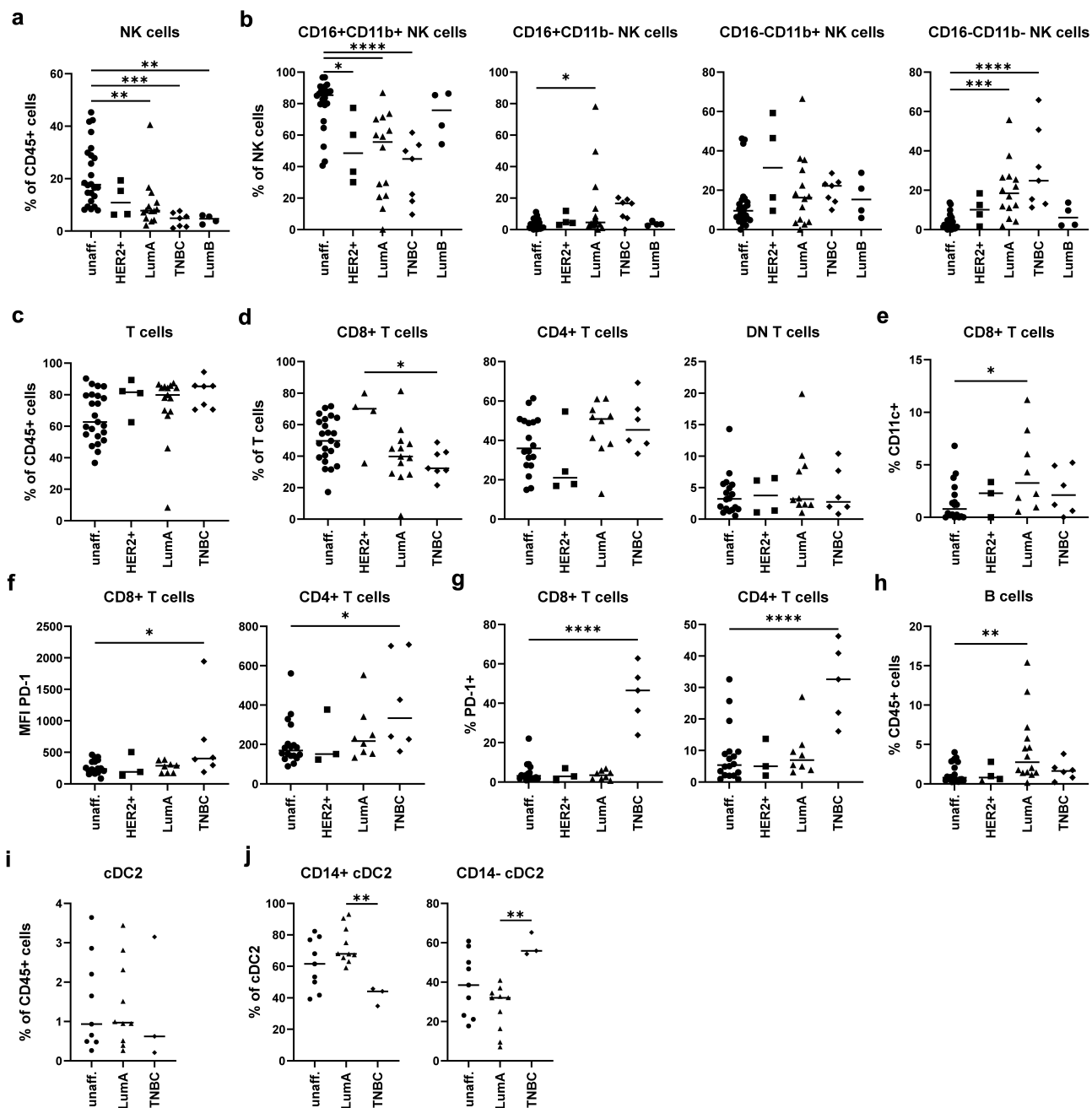


Figure 5. Validation of the identified alterations in the NK cell, T cell, B cell, and cDC2 compartment using a second cohort of BC patients. In order to validate the identified alterations using the unbiased approach, NK cells, T cells, B cells, and cDC2 were analyzed in the samples of the first cohort and in additional donors of a second cohort. Cells were gated according to Figure S5. a) Frequency of NK cells among CD45⁺ immune cells was determined. b) NK cells were analyzed for expression of CD16 as well as CD11b and distinguished into CD16⁺CD11b⁺ cells, CD16⁺CD11b⁻ cells, CD16⁻CD11b⁺ cells, and CD16⁻CD11b⁻ cells. c) Frequency of CD3⁺ T cells among CD45⁺ immune cells was determined. d) CD3⁺ T cells were distinguished into CD4⁺, CD8⁺, and DN T cells and frequency among T cells was determined. e) Shown is the frequency of CD11c⁺ cells among CD8⁺ T cells. f) MFI value for PD-1 expression and g) percentage of PD-1⁺ cells was determined for each T cell population. h) the frequency of B cells was determined for each sample. i) The frequency of cDC2 among all CD45⁺ immune cells was determined for each sample with more than 50 cDC2 in the final gate (Figure S5C) as well as j) the phenotype based on CD14 expression. a-j) the frequency or MFI value were plotted as scatter plot (one-way ANOVA with Dunnett's multiple comparison test; **p* < 0.05, ***p* < 0.01, ****p* < 0.001, *****p* < 0.0001).

CD36, CD163, or CD14 dependent on the study^{26–31}. As CD14⁺ cDC2, corresponding to DC3, are reported to be enriched in tumor patients, we divided cDC2 into CD14⁺ and CD14⁻ cDC2 (Figure S5C). Notably, the phenotype of cDC2 differed between Luminal A-type and TNBC as CD14⁺ cDC2 were enriched in Luminal A-type BC, while TNBC showed an enrichment of CD14⁻ cDC2 (Figure 5j).

Overall, we determined specific immune cell signatures for different subtypes of BC by using high-dimensional flow cytometry followed by UMAP and X-Shift clustering. Thereby, we could identify a reduction in CD11b⁺CD16⁺ NK cells in Luminal A- and B-type BC as well as in TNBC. Further, TNBC showed a specific expression of the exhaustion marker PD-1 on CD4⁺ and CD8⁺ T cells. Lastly, Luminal A-type and

TNBC differed in the composition of the cDC2 subsets DC2 and DC3.

Discussion

BC is a highly heterogeneous disease as several molecular subtypes exist^{24,32}. It is widely accepted that infiltrating lymphocytes are positively associated with pathological complete response (pCR) as well as overall survival^{2,5}. While analysis of lymphocyte infiltration or even large cell populations, such as T cells, is possible by standardized methods such as immunohistochemistry, quantitative real-time PCR, or bulk RNA-sequencing, identification of complex cell populations is hardly possible. Here, we presented a workflow for the analysis of the immune cell compartment in BC samples to identify changes in the immune cell signature which might have an influence on the response to immunotherapies such as blockade of checkpoint molecules (e.g. PD-1)³³. Thereby, we determined subtype-specific changes in the frequency and the phenotype of T cells, NK cells, B cells, and in the DC compartment (Figure 5). However, we cannot exclude that inflammation and wound healing processes induced by the diagnostic biopsy prior to the surgery might have influenced the immune cell signature determined in our study, which relied on tumor material removed during surgery. Due to the small size of the pre-surgery biopsy, high-dimensional flow cytometric analysis was only possible with larger specimens obtained during surgery. However, the infiltration of the tumor tissue with CD45⁺ immune cells was comparable to published data on TILs determined in pre-surgery diagnostic biopsies^{5,6,8}.

NK cells are crucial effector cells for the killing of tumor cells and presence of NK cells in the tumor is associated with good prognosis in BC^{16,17,34–36}. However, our data revealed that the ratio of NK cells was significantly lower in BC tissue compared to surrounding unaffected breast tissue, and they showed markedly lower expression of CD11b and CD16 (Figure 3–5). In general, CD11b⁺ and CD16⁺ NK cells represent cytotoxic NK cells, while CD11b[−] and CD16[−] rather resemble regulatory NK cells^{34,37}. In accordance with our data, others also found CD56^{bright}CD16^{low} NK cells in solid tumors, such as BC^{38–40}. As the tumor seems to evade NK cell responses, it might be beneficial for patients to prevent immunosuppression of NK cells by the tumor. As shown in Figure 2, our data revealed that neoadjuvant chemotherapy increased the percentage of cytotoxic CD11b⁺CD16⁺ NK cells compared to untreated BC patients. Due to the small size of pre-surgery core biopsies, we could not verify the changes in the same patient but had to compare treated with untreated BC patients. In accordance with our data, Ladoire et al. showed similar positive effects of neoadjuvant chemotherapy on the infiltration of breast cancer with Th1 cells⁴¹. Several pathways have been shown to suppress NK cells in the tumor microenvironment, such as TGFβ produced by tumor cells^{42,43}, COX-2-dependent production of PGE₂¹⁶, and expression of HLA-G and HLA-I molecules on BC cells^{44–46}. Thus, interfering with these pathways might boost NK cell-mediated anti-tumor responses. Additional pathways might exist how tumors such as BC interfere with NK cells.

Therefore, further research needs to be done to uncover these pathways in order to develop new treatment strategies for BC.

We also observed changes in the DC compartment in Luminal A-type and TNBC (Figures 3–5). While TNBC harbored rather CD14[−] cDC2, also termed DC2, Luminal A-type BC was enriched for CD14⁺ cDC2, also termed DC3 (Figure 5). Thus, Luminal A-type and TNBC differed in the composition of the DC compartment, which might be involved in the worse prognosis of TNBC^{3,4}. CD14⁺ DC3 were first identified in melanomas and shown to overexpress PD-L1 and to only weakly induce T cell proliferation²⁶. In Luminal breast cancer, the frequency of DC3 was positively associated with the presence of CD69⁺ tissue-resident memory CD8⁺ T cells, which might be responsible for the better prognosis of Luminal A-type BC patients³⁰. However, in a human organotypic melanoma culture model, melanoma cells induced differentiation of CD14[−] cDC2 into pro-tumorigenic CD14⁺ DC3 expressing lower level of co-stimulatory molecules but higher amounts of PD-L1 and markers of tumor-associated macrophages⁴⁷. Further studies need to clarify the functional properties of DC subpopulations in different BC subtypes. In this regard, Michea et al. performed RNA-seq analysis of enriched or purified DC subpopulations of Luminal and TNBC⁴⁸. Their data suggest that DCs in TNBC display an enrichment for genes of the interferon pathway implying an activated phenotype of DCs in TNBC⁴⁸. However, enrichment for the signature of cDC2 in bulk RNA-seq data of breast cancer patients was only associated with longer disease-free survival in Luminal but not in TNBC⁴⁸. In addition, functional as well as correlation data demonstrate that the presence of cDC1 in BC and other solid tumors is important for improved survival of the patients as they are directly recruited by NK cells^{16,17}. In contrast to cDC2, presence of cDC1 was shown in both Luminal and TNBC to be positively associated with disease-free survival of the patients⁴⁸. In addition, we observed that B cells were enriched in Luminal A-type BC (Figure 3 and 5). In HER2-enriched BC, higher numbers of B cells are associated with decreased survival⁴⁹, while proliferative response of B cells in TNBC under ICB is a predictor for pCR⁵⁰. Whether B cells are involved in the general good prognosis of Luminal A-type BC is unclear and has to be tested in future studies.

While we did not observe general differences in the T cell compartment in BC compared to unaffected surrounding tissue, we detected specific expression of PD-1 on CD4⁺ and CD8⁺ T cells in TNBC (Figures 3–5). PD-1 is described as a marker for exhausted T cells and contributes to immune evasion by different mechanisms. On the one hand, PD-1 leads to TCR internalization on T cells, reduction of cytokine secretion and cytotoxicity as well as induction of apoptosis in T cells^{51–54}. On the other hand, PD-L1 expression on tumor cells is pro-tumorigenic as it prevents IFN-induced cytotoxicity⁵⁵. In addition to PD-1, Wu et al. observed LAG-3 expression on CD8⁺ T cells in TNBC by performing CITE-seq⁵⁶. In accordance with our data, PD-L1 is overexpressed especially on BC cells in TNBC¹⁹. Interestingly, overexpression of PD-1 on T cells in TNBC is associated with improved disease-free survival^{57,58}. However, it is not fully understood how exhausted T cells positively influence

survival of the patients, yet. Recently, PD-1⁺ Tcf1⁺ CD8⁺ stem-like T cells were described that were the main responders to checkpoint therapy and resulted in differentiation into tumor-reactive effector cells^{59,60}. Whether the observed PD-1⁺ T cells in TNBC correspond to these stem-like T cells has to be tested in future studies. Further, we observed enrichment of CD11c⁺CD8⁺ T cells in Luminal A-type BC. CD11c⁺CD8⁺ T cells were identified both in mice and men^{61–65}. However, their function seems to depend on the environment as they were described both as regulatory as well as with high effector functions. Further studies are needed to elucidate the function of the identified CD11c⁺CD8⁺ T cells in Luminal A-type BC and to determine whether they are involved in the beneficial prognosis of Luminal A-type BC compared to HER2-enriched as well as TNBC.

Acknowledgments

Funding: The study was funded by the Emerging Fields Initiative BIG-THERA to FN, TB, AM, PF, and MWB with DD as speaker and coordinator (FAU Erlangen-Nürnberg, Staedtler Stiftung). DD was funded by the German Research Foundation [Deutsche Forschungsgemeinschaft (DFG)] (DU548/5-1 420943261, TRR305-B05 429280966) and a proposal funded by the Agence Nationale de la Recherche (ANR) and the DFG (DU548/6-1 431402787). FN was funded by TRR305-B02, AH and PF were funded by TRR305-Z02 429280966, and TB received funding from TRR305-Z01 429280966.

Disclosure statement

No potential conflict of interest was reported by the author(s).

Funding

The work was supported by the Deutsche Forschungsgemeinschaft [TRR305-B02]; Deutsche Forschungsgemeinschaft [TRR305-Z01]; Deutsche Forschungsgemeinschaft [DU548/5-1 420943261, TRR305-Z02, TRR305-B05 429280966]; Friedrich-Alexander-Universität Erlangen-Nürnberg [Emerging Fields Initiative BIG-THERA]; Agence Nationale de la Recherche and Deutsche Forschungsgemeinschaft [DU548/6-1 431402787]; Staedtler Stiftung [Emerging Fields Initiative BIG-THERA].

Author contributions

Lukas Heger performed the experiments with the participation of Gordon F. Heidkamp and Lukas Amon. Matthias Rübner, Caroline C. Hack, Hanna Huebner, Ramona Erber, Peter Fasching, and Matthias W. Beckmann gave scientific advice and were responsible for supply with human breast cancer tissue, grading, and molecular subtype characterization. Falk Nimmerjahn, Tobias Bäuerle and Andreas Maier provided valuable scientific advice and data interpretation. Lukas Heger and Diana Dudziak analyzed the data. Lukas Heger and Diana Dudziak supervised and designed the study. Lukas Heger and Diana Dudziak wrote the manuscript with contributions from all authors.

Data availability statement

The data supporting this study are available from the corresponding authors upon reasonable request.

References

1. Harbeck N, Gnant M. Breast cancer. *Lancet*. 2017;389(10074):1134–1150. doi: [10.1016/S0140-6736\(16\)31891-8](https://doi.org/10.1016/S0140-6736(16)31891-8).
2. Denkert C, von Minckwitz G, Darb-Esfahani S, Lederer B, Heppner BI, Weber KE, Budczies J, Huober J, Klauschen F, Furlanetto J, et al. Tumour-infiltrating lymphocytes and prognosis in different subtypes of breast cancer: a pooled analysis of 3771 patients treated with neoadjuvant therapy. *Lancet Oncol*. 2018;19(1):40–50. doi: [10.1016/S1470-2045\(17\)30904-X](https://doi.org/10.1016/S1470-2045(17)30904-X).
3. Carey LA, Perou CM, Livasy CA, Dressler LG, Cowan D, Conway K, Karaca G, Troester MA, Tse CK, Edmiston S, et al. 2006. Race, breast cancer subtypes, and survival in the Carolina breast cancer study. *JAMA*. 295(21):2492. doi: [10.1001/jama.295.21.2492](https://doi.org/10.1001/jama.295.21.2492).
4. Howlander N, Cronin KA, Kurian AW, Andridge R. Differences in breast cancer survival by molecular subtypes in the United States. *Cancer Epidemiol Biomarkers Prev*. 2018;27(6):619–626. doi: [10.1158/1055-9965.EPI-17-0627](https://doi.org/10.1158/1055-9965.EPI-17-0627).
5. Denkert C, Loibl S, Noske A, Roller M, Müller BM, Komor M, Budczies J, Darb-Esfahani S, Kronenwett R, Hanusch C, et al. Tumor-associated lymphocytes as an independent predictor of response to neoadjuvant chemotherapy in breast cancer. *J Clin Oncol*. 2010;28(1):105–113. doi: [10.1200/JCO.2009.23.7370](https://doi.org/10.1200/JCO.2009.23.7370).
6. Loi S, Sirtaine N, Piette F, Salgado R, Viale G, Van Eeno F, Rouas G, Francis P, Crown JPA, Hitre E, et al. Prognostic and predictive value of tumor-infiltrating lymphocytes in a phase III randomized adjuvant breast cancer trial in node-positive breast cancer comparing the addition of docetaxel to doxorubicin with doxorubicin-based chemotherapy: BIG 02-98. *J Clin Oncol*. 2013;31(7):860–867. doi: [10.1200/JCO.2011.41.0902](https://doi.org/10.1200/JCO.2011.41.0902).
7. Würfel F, Erber R, Huebner H, Hein A, Lux MP, Jud S, Kremer A, Kranich H, Mackensen A, Häberle L, et al. 2018. Tilgen: a program to investigate immune targets in breast cancer patients - first results on the influence of tumor-infiltrating lymphocytes. *Breast Care*. 13(1):8–14. doi: [10.1159/000486949](https://doi.org/10.1159/000486949).
8. Stanton SE, Adams S, Disis ML. Variation in the incidence and magnitude of tumor-infiltrating lymphocytes in breast cancer subtypes: a systematic review. *JAMA Oncol*. 2016;2(10):1354–1360. doi: [10.1001/jamaoncol.2016.1061](https://doi.org/10.1001/jamaoncol.2016.1061).
9. Loi S, Michiels S, Adams S, Loibl S, Budczies J, Denkert C, Salgado R. The journey of tumor-infiltrating lymphocytes as a biomarker in breast cancer: clinical utility in an era of checkpoint inhibition. *Ann Oncol*. 2021;32(10):1236–1244. doi: [10.1016/j.annonc.2021.07.007](https://doi.org/10.1016/j.annonc.2021.07.007).
10. Kristensen VN, Vaske CJ, Ursini-Siegel J, Van Loo P, Nordgard SH, Sachidanandam R, Sørli T, Wärnberg F, Haakensen VD, Helland Å, et al. Integrated molecular profiles of invasive breast tumors and ductal carcinoma in situ (DCIS) reveal differential vascular and interleukin signaling. *Proc Natl Acad Sci U S A*. 2012;109(8):2802–2807. doi: [10.1073/pnas.1108781108](https://doi.org/10.1073/pnas.1108781108).
11. Bates GJ, Fox SB, Han C, Leek RD, Garcia JF, Harris AL, Banham AH. Quantification of regulatory T cells enables the identification of high-risk breast cancer patients and those at risk of late relapse. *J Clin Oncol*. 2006;24(34):5373–5380. doi: [10.1200/JCO.2006.05.9584](https://doi.org/10.1200/JCO.2006.05.9584).
12. Baker K, Lachapelle J, Zlobec I, Bismar TA, Terracciano L, Foulkes WD. Prognostic significance of CD8+ T lymphocytes in breast cancer depends upon both oestrogen receptor status and histological grade. *Histopathology*. 2011;58(7):1107–1116. doi: [10.1111/j.1365-2559.2011.03846.x](https://doi.org/10.1111/j.1365-2559.2011.03846.x).
13. Liu S, Lachapelle J, Leung S, Gao D, Foulkes WD, Nielsen TO. CD8+lymphocyte infiltration is an independent favorable prognostic indicator in basal-like breast cancer. *Breast Cancer Res*. 2012;14(2). doi: [10.1186/bcr3148](https://doi.org/10.1186/bcr3148).
14. Liu F, Lang R, Zhao J, Zhang X, Pringle GA, Fan Y, Yin D, Gu F, Yao Z, Fu L. CD8+ cytotoxic T cell and FOXP3+ regulatory T cell infiltration in relation to breast cancer survival and molecular subtypes. *Breast Cancer Res Treat*. 2011;130(2):645–655. doi: [10.1007/s10549-011-1647-3](https://doi.org/10.1007/s10549-011-1647-3).

15. Mao Y, Qu Q, Zhang Y, Liu J, Chen X, Shen K, Beck AH. The value of tumor infiltrating lymphocytes (TILs) for predicting response to neoadjuvant chemotherapy in breast cancer: a systematic review and meta-analysis. *PLoS ONE*. 2014;9(12):1–21. doi: [10.1371/journal.pone.0115103](https://doi.org/10.1371/journal.pone.0115103).
16. Böttcher JP, Bonavita E, Chakravarty P, Brees H, Cabeza-Cabrero M, Sannichelli S, Rogers NC, Sahai E, Zelenay S, Reis e Sousa C. NK cells Stimulate Recruitment of cDC1 into the tumor microenvironment promoting cancer immune control. *Cell*. 2018;172(5):1022–1028.e14. doi: [10.1016/j.cell.2018.01.004](https://doi.org/10.1016/j.cell.2018.01.004).
17. Barry KC, Hsu J, Broz ML, Cueto FJ, Binnewies M, Combes AJ, Nelson AE, Loo K, Kumar R, Rosenblum MD, et al. 2018. A natural killer–dendritic cell axis defines checkpoint therapy–responsive tumor microenvironments. *Nat Med*. 24(8):1178–1191. doi: [10.1038/s41591-018-0085-8](https://doi.org/10.1038/s41591-018-0085-8).
18. Thompson E, Taube JM, Elwood H, Sharma R, Meeker A, Warzecha HN, Argani P, Cimino-Mathews A, Emens LA. The immune microenvironment of breast ductal carcinoma in situ. *Mod Pathol*. 2016;29(3):249–258. doi: [10.1038/modpathol.2015.158](https://doi.org/10.1038/modpathol.2015.158).
19. Mittendorf EA, Philips AV, Meric-Bernstam F, Qiao N, Wu Y, Harrington S, Su X, Wang Y, Gonzalez-Angulo AM, Akcakanat A, et al. 2014. PD-L1 expression in triple-negative breast cancer. *Cancer Immunol Res*. 2(4):361–370. doi: [10.1158/2326-6066.CIR-13-0127](https://doi.org/10.1158/2326-6066.CIR-13-0127).
20. Adams S, Gray RJ, Demaria S, Goldstein L, Perez EA, Shulman LN, Martino S, Wang M, Jones VE, Saphner TJ, et al. Prognostic value of tumor-infiltrating lymphocytes in triple-negative breast cancers from two phase III randomized adjuvant breast cancer trials: ECOG 2197 and ECOG 1199. *J Clin Oncol*. 2014;32(27):2959–2966. doi: [10.1200/JCO.2013.55.0491](https://doi.org/10.1200/JCO.2013.55.0491).
21. McInnes L, Healy J, Melville J, Großberger L. UMAP: uniform manifold approximation and projection for dimension reduction. *J Open Source Softw*. 2018 Feb 9;3(29):861. doi: [10.21105/joss.00861](https://doi.org/10.21105/joss.00861).
22. Samusik N, Good Z, Spitzer MH, Davis KL, Nolan GP. Automated mapping of phenotype space with single-cell data. *Nat Methods*. 2016;13(6):493–496. doi: [10.1038/nmeth.3863](https://doi.org/10.1038/nmeth.3863).
23. Prat A, Pineda E, Adamo B, Galván P, Fernández A, Gaba L, Diez M, Viladot M, Arance A, Muñoz M. Clinical implications of the intrinsic molecular subtypes of breast cancer. *Breast*. 2015;24:S26–S35. doi: [10.1016/j.breast.2015.07.008](https://doi.org/10.1016/j.breast.2015.07.008).
24. Zardavas D, Irrthum A, Swanton C, Piccart M. Clinical management of breast cancer heterogeneity. *Nat Rev Clin Oncol*. 2015;12(7):381–394. doi: [10.1038/nrclinonc.2015.73](https://doi.org/10.1038/nrclinonc.2015.73).
25. Krijgsman D, Hokland M, Kuppen PJK. The role of natural killer T cells in cancer—A phenotypical and functional approach. *Front Immunol*. 2018;9(FEB). doi: [10.3389/fimmu.2018.00367](https://doi.org/10.3389/fimmu.2018.00367).
26. Bakdash G, Buschow SI, Gorris MAJ, Halilovic A, Hato SV, Sköld AE, Schreibelt G, Sittig SP, Torensma R, Duiveman-De Boer T, et al. 2016. Expansion of a BDCA1+ CD14+ myeloid cell population in melanoma patients may attenuate the efficacy of dendritic cell vaccines. *Cancer Res*. 76(15):4332–4346. doi: [10.1158/0008-5472.CAN-15-1695](https://doi.org/10.1158/0008-5472.CAN-15-1695).
27. Villani A-C, Satija R, Reynolds G, Sarkizova S, Shekhar K, Fletcher J, Griesbeck M, Butler A, Zheng S, Lazo S, et al. 2017. Single-cell RNA-seq reveals new types of human blood dendritic cells, monocytes, and progenitors. *Science* (80-). 356(6335): eaah4573. doi: [10.1126/science.aah4573](https://doi.org/10.1126/science.aah4573).
28. Dutertre CA, Becht E, Irac SE, Khalilnezhad A, Narang V, Khalilnezhad S, Ng PY, van den Hoogen LL, Leong JY, Lee B, et al. 2019. Single-cell analysis of human mononuclear phagocytes reveals subset-defining markers and identifies circulating inflammatory dendritic cells. *Immunity*. 51(3):573–589.e8. doi: [10.1016/j.immuni.2019.08.008](https://doi.org/10.1016/j.immuni.2019.08.008).
29. Santegoets SJ, Duurland CL, Jordanova EJ, van Ham VJ, Ehsan I, Loof NM, Narang V, Dutertre CA, Ginhoux F, van Egmond SL, et al. CD163+ cytokine-producing cDC2 stimulate intratumoral type 1 T cell responses in HPV16-induced oropharyngeal cancer. *J Immunother Cancer*. 2020;8(2):1–15. doi: [10.1136/jitc-2020-001053](https://doi.org/10.1136/jitc-2020-001053).
30. Bourdely P, Anselmi G, Vaivode K, Ramos RN, Missolo-Koussou Y, Hidalgo S, Tosselo J, Nuñez N, Richer W, Vincent-Salomon A, et al. Transcriptional and functional analysis of CD1c+ human dendritic cells Identifies a CD163+ subset priming CD8+CD103+ T cells. *Immunity*. 2020;1–18. doi: [10.1016/j.immuni.2020.06.002](https://doi.org/10.1016/j.immuni.2020.06.002).
31. Heger L, Hofer TP, Bigley V, de Vries IJM, Dalod M, Dudziak D, Ziegler-Heitbrock L. Subsets of CD1c+ DCs: dendritic cell versus monocyte lineage. *Front Immunol*. 2020;11(September):1–11. doi: [10.3389/fimmu.2020.559166](https://doi.org/10.3389/fimmu.2020.559166).
32. Lichert F. Histologische Typen bei triple-negativem Brustkrebs charakterisiert. *Geburtshilfe Frauenheilkd*. 2023;83(3):234–235. doi: [10.1055/a-1985-2161](https://doi.org/10.1055/a-1985-2161).
33. Würstlein R, Harbeck N. Immuntherapie bei Brustkrebs. *Geburtshilfe Frauenheilkd*. 2021;81(3):255–259. doi: [10.1055/a-1071-6595](https://doi.org/10.1055/a-1071-6595).
34. Bald T, Krummel MF, Smyth MJ, Barry KC. The NK cell–cancer cycle: advances and new challenges in NK cell–based immunotherapies. *Nat Immunol*. 2020;21(8):835–847. doi: [10.1038/s41590-020-0728-z](https://doi.org/10.1038/s41590-020-0728-z).
35. Jacobs B, Gebel V, Heger L, Grèze V, Schild H, Dudziak D, Ullrich E. Characterization and manipulation of the crosstalk between dendritic and natural killer cells within the tumor microenvironment. *Front Immunol*. 2021;12(May):1–11. doi: [10.3389/fimmu.2021.670540](https://doi.org/10.3389/fimmu.2021.670540).
36. Muntasell A, Rojo F, Servitja S, Rubio-Perez C, Cabo M, Tamborero D, Costa-García M, Martínez-García M, Menendez S, Vazquez I, et al. NK cell infiltrates and HLA class I expression in primary HER2 β breast cancer predict and uncouple pathological response and disease-free survival. *Clin Cancer Res*. 2019;25(5):1535–1545. doi: [10.1158/1078-0432.CCR-18-2365](https://doi.org/10.1158/1078-0432.CCR-18-2365).
37. Wu SY, Fu T, Jiang YZ, Shao ZM. Natural killer cells in cancer biology and therapy. *Mol Cancer*. 2020;19(1):1–26. doi: [10.1186/s12943-020-01238-x](https://doi.org/10.1186/s12943-020-01238-x).
38. Carrega P, Bonaccorsi I, Di Carlo E, Morandi B, Paul P, Rizzello V, Cipollone G, Navarra G, Mingari MC, Moretta L, et al. CD56 bright perforin low Noncytotoxic human NK cells are abundant in both healthy and Neoplastic solid Tissues and recirculate to secondary lymphoid organs via Afferent Lymph. *J Immunol*. 2014;192(8):3805–3815. doi: [10.4049/jimmunol.1301889](https://doi.org/10.4049/jimmunol.1301889).
39. Carrega P, Morandi B, Costa R, Frumento G, Forte G, Altavilla G, Ratto GB, Mingari MC, Moretta L, Ferlazzo G. Natural killer cells infiltrating human nonsmall-cell lung cancer are enriched in CD56brightCD16– cells and display an impaired capability to kill tumor cells. *Cancer*. 2008;112(4):863–875. doi: [10.1002/ncr.23239](https://doi.org/10.1002/ncr.23239).
40. Mamessier E, Sylvain A, Bertucci F, Castellano R, Finetti P, Houvenaeghel G, Charaffe-Jaufret E, Birnbaum D, Moretta A, Olive D. Human breast tumor cells induce self-tolerance mechanisms to avoid NKG2D-mediated and DNAM-mediated NK cell recognition. *Cancer Res*. 2011;71(21):6621–6632. doi: [10.1158/0008-5472.CAN-11-0792](https://doi.org/10.1158/0008-5472.CAN-11-0792).
41. Ladoire S, Arnould L, Mignot G, Apetoh L, Rébé C, Martin F, Fumoleau P, Coudert B, Ghiringhelli F. T-bet expression in intratumoral lymphoid structures after neoadjuvant trastuzumab plus docetaxel for HER2-overexpressing breast carcinoma predicts survival. *Br J Cancer*. 2011;105(3):366–371. doi: [10.1038/bjc.2011.261](https://doi.org/10.1038/bjc.2011.261).
42. Slattery K, Woods E, Zaiatz-Bittencourt V, Marks S, Chew S, Conroy M, Goggin C, Maceochagain C, Kennedy J, Lucas S, et al. TGF β drives NK cell metabolic dysfunction in human metastatic breast cancer. *J Immunother Cancer*. 2021;9(2):e002044. doi: [10.1136/jitc-2020-002044](https://doi.org/10.1136/jitc-2020-002044).
43. Krneta T, Gillgrass A, Chew M, Ashkar AA. The breast tumor microenvironment alters the phenotype and function of natural killer cells. *Cell Mol Immunol*. 2016;13(5):628–639. doi: [10.1038/cmi.2015.42](https://doi.org/10.1038/cmi.2015.42).
44. Morel E, Bellon T. HLA class I molecules regulate IFN- γ production induced in NK cells by Target cells, viral products, or immature dendritic cells through the inhibitory receptor ILT2/CD85j. *J Immunol*. 2008;181(4):2368–2381. doi: [10.4049/jimmunol.181.4.2368](https://doi.org/10.4049/jimmunol.181.4.2368).
45. Roberti MP, Juliá EP, Rocca YS, Amat M, Bravo AI, Loza J, Coló F, Loza CM, Fabiano V, Maino M, et al. 2015. Overexpression of

- CD85j in TNBC patients inhibits Cetuximab-mediated NK-cell ADCC but can be restored with CD85j functional blockade. *Eur J Immunol.* 45(5):1560–1569. doi: [10.1002/eji.201445353](https://doi.org/10.1002/eji.201445353).
46. Favier B, LeMaout J, Lesport E, Carosella ED. ILT2/HLA-G interaction impairs NK-cell functions through the inhibition of the late but not the early events of the NK-cell activating synapse. *FASEB J.* 2010;24(3):689–699. doi: [10.1096/fj.09-135194](https://doi.org/10.1096/fj.09-135194).
 47. Di Blasio S, van Wigcheren GF, Becker A, van Duffelen A, Gorris M, Verrijp K, Stefanini I, Bakker GJ, Bloemendal M, Halilovic A, et al. The tumour microenvironment shapes dendritic cell plasticity in a human organotypic melanoma culture. *Nat Commun.* 2020;11(1):1–17. doi: [10.1038/s41467-020-16583-0](https://doi.org/10.1038/s41467-020-16583-0).
 48. Michea P, Noël F, Zakine E, Czerwinska U, Sirven P, Abouzid O, Goudot C, Scholer-Dahirel A, Vincent-Salomon A, Reyat F, et al. Adjustment of dendritic cells to the breast-cancer microenvironment is subset specific. *Nat Immunol.* 2018;19(8):885–897. doi: [10.1038/s41590-018-0145-8](https://doi.org/10.1038/s41590-018-0145-8).
 49. Steenbruggen TG, Wolf DM, Campbell MJ, Sanders J, Cornelissen S, Thijssen B, Salgado RA, Yau C, O-Grady N, Basu A, et al. 2023. B-cells and regulatory T-cells in the microenvironment of HER2+ breast cancer are associated with decreased survival: a real-world analysis of women with HER2+ metastatic breast cancer. *Breast Cancer Res.* 25(1):1–19. doi: [10.1186/s13058-023-01717-1](https://doi.org/10.1186/s13058-023-01717-1).
 50. Wang XQ, Danenberg E, Huang CS, Egle D, Callari M, Bermejo B, Dugo M, Zamagni C, Thill M, Anton A, et al. Spatial predictors of immunotherapy response in triple-negative breast cancer. *Nature.* 2023;621(September):868–876. doi: [10.1038/s41586-023-06498-3](https://doi.org/10.1038/s41586-023-06498-3).
 51. Freeman GJ, Long AJ, Iwai Y, Bourque K, Chernova T, Nishimura H, Fitz LJ, Malenkovich N, Okazaki T, Byrne MC, et al. Engagement of the PD-1 immunoinhibitory receptor by a novel B7 family member leads to negative regulation of lymphocyte activation. *J Exp Med.* 2000;192(7):1027–1034. doi: [10.1084/jem.192.7.1027](https://doi.org/10.1084/jem.192.7.1027).
 52. Dong H, Strome SE, Salomao DR, Tamura H, Hirano F, Flies DB, Roche PC, Lu J, Zhu G, Tamada K, et al. 2002. Tumor-associated B7-H1 promotes T-cell apoptosis: a potential mechanism of immune evasion. *Nat Med.* 8(8):793–800. doi: [10.1038/nm730](https://doi.org/10.1038/nm730).
 53. Karwacz K, Bricogne C, MacDonald D, Arce F, Bennett CL, Collins M, Escors D. PD-L1 co-stimulation contributes to ligand-induced T cell receptor down-modulation on CD8 + T cells. *EMBO Mol Med.* 2011;3(10):581–592. doi: [10.1002/emmm.201100165](https://doi.org/10.1002/emmm.201100165).
 54. Latchman YE, Liang SC, Wu Y, Chernova T, Sobel RA, Klemm M, Kuchroo VK, Freeman GJ, Sharpe AH. PD-L1-deficient mice show that PD-L1 on T cells, antigen-presenting cells, and host tissues negatively regulates T cells. *Proc Natl Acad Sci.* 2004;101(29):10691–10696. doi: [10.1073/pnas.0307252101](https://doi.org/10.1073/pnas.0307252101).
 55. Gato-Cañas M, Zuazo M, Arasanz H, Ibañez-Vea M, Lorenzo L, Fernandez-Hinojal G, Vera R, Smerdou C, Martisova E, Arozarena I, et al. PDL1 signals through conserved sequence motifs to overcome interferon-mediated cytotoxicity. *Cell Rep.* 2017;20(8):1818–1829. doi: [10.1016/j.celrep.2017.07.075](https://doi.org/10.1016/j.celrep.2017.07.075).
 56. Wu SZ, Al-Eryani G, Roden DL, Junankar S, Harvey K, Andersson A, Thennavan A, Wang C, Torpy JR, Bartonicek N, et al. 2021. A single-cell and spatially resolved atlas of human breast cancers. *Nat Genet.* 53(9):1334–1347. doi: [10.1038/s41588-021-00911-1](https://doi.org/10.1038/s41588-021-00911-1).
 57. Ren X, Wu H, Lu J, Zhang Y, Luo Y, Xu Q, Shen S, Liang Z. PD1 protein expression in tumor infiltrated lymphocytes rather than PDL1 in tumor cells predicts survival in triple-negative breast cancer. *Cancer Biol Ther.* 2018;19(5):373–380. doi: [10.1080/15384047.2018.1423919](https://doi.org/10.1080/15384047.2018.1423919).
 58. Yeong J, Lim JCT, Lee B, Li H, Ong CCH, Thike AA, Yeap WH, Yang Y, Lim AYH, Tay TKY, et al. Prognostic value of CD8 + PD-1 + immune infiltrates and PDCD1 gene expression in triple negative breast cancer. *J Immunother Cancer.* 2019;7(1):1–13. doi: [10.1186/s40425-019-0499-y](https://doi.org/10.1186/s40425-019-0499-y).
 59. Codarri Deak L, Nicolini V, Hashimoto M, Karagianni M, Schwalie PC, Lauener L, Varypataki EM, Richard M, Bommer E, Sam J, et al. 2022. PD-1-cis IL-2R agonism yields better effectors from stem-like CD8+ T cells. *Nature.* 610(7930):161–172. doi: [10.1038/s41586-022-05192-0](https://doi.org/10.1038/s41586-022-05192-0).
 60. Siddiqui I, Schaeuble K, Chennupati V, Fuertes Marraco SA, Calderon-Copete S, Pais Ferreira D, Carmona SJ, Scarpellino L, Gfeller D, Pradervand S, et al. Intratumoral Tcf1 + PD-1 + CD8 + T cells with stem-like properties promote tumor control in response to vaccination and checkpoint blockade immunotherapy. *Immunity.* 2019;50(1):195–211.e10. doi: [10.1016/j.immuni.2018.12.021](https://doi.org/10.1016/j.immuni.2018.12.021).
 61. Vinay DS, Kwon BS. CD11c+CD8+ T cells: Two-faced adaptive immune regulators. *Cell Immunol.* 2010;264(1):18–22. doi: [10.1016/j.cellimm.2010.05.010](https://doi.org/10.1016/j.cellimm.2010.05.010).
 62. Vinay DS, Kim CH, Choi BK, Kwon BS. Origins and functional basis of regulatory CD11c+CD8+ T cells. *Eur J Immunol.* 2009;39(6):1552–1563. doi: [10.1002/eji.200839057](https://doi.org/10.1002/eji.200839057).
 63. Beyer M, Wang H, Peters N, Doths S, Koerner-Rettberg C, Openshaw PJM, Schwarze J. The beta2 integrin CD11c distinguishes a subset of cytotoxic pulmonary T cells with potent antiviral effects in vitro and in vivo. *Respir Res.* 2005;6(1):1–11. doi: [10.1186/1465-9921-6-70](https://doi.org/10.1186/1465-9921-6-70).
 64. Qualai J, Li LX, Cantero J, Tarrats A, Fernández MA, Sumoy L, Rodoloso A, McSorley SJ, Genescà M, Reeves RK. Expression of CD11c is associated with unconventional activated T cell subsets with high migratory potential. *PLoS ONE.* 2016;11(4):1–22. doi: [10.1371/journal.pone.0154253](https://doi.org/10.1371/journal.pone.0154253).
 65. Takeda Y, Azuma M, Matsumoto M, Seya T. Tumoricidal efficacy coincides with CD11c up-regulation in antigen-specific CD8+ T cells during vaccine immunotherapy. *J Exp Clin Cancer Res.* 2016;35(1):1–16. doi: [10.1186/s13046-016-0416-x](https://doi.org/10.1186/s13046-016-0416-x).